Mechanism of DNA Polymerization Catalyzed by *Sulfolobus solfataricus* P2 DNA Polymerase IV†

Kevin A. Fiala‡ and Zucai Suo*,‡,§

Department of Biochemistry, Ohio State Biochemistry Program, Ohio State Biophysics Program, Molecular, Cellular and Developmental Biology Program, and Comprehensive Cancer Center, The Ohio State University, Columbus, Ohio 43210

Received September 26, 2003; Revised Manuscript Received December 23, 2003

ABSTRACT: The kinetic mechanism of DNA polymerization catalyzed by *Sulfolobus solfataricus* P2 DNA polymerase IV (Dpo4) is resolved by pre-steady-state kinetic analysis of single-nucleotide (dTTP) incorporation into a DNA 21/41-mer. Like replicative DNA polymerases, Dpo4 utilizes an "induced-fit" mechanism to select correct incoming nucleotides. The affinity of DNA and a matched incoming nucleotide for Dpo4 was measured to be 10.6 nM and 230 μM, respectively. Dpo4 binds DNA with an affinity similar to that of replicative polymerases due to the presence of an atypical little finger domain and a highly charged tether that links this novel domain to its small thumb domain. On the basis of the elemental effect between the incorporations of dTTP and its thio analogue S_p-dTTPαS, the incorporation of a correct incoming nucleotide by Dpo4 was shown to be limited by the protein conformational change step preceding the chemistry step. In contrast, the chemistry step limited the incorporation of an incorrect nucleotide. The measured dissociation rates of the enzyme·DNA binary complex (0.02−0.07 s^{-1}), the enzyme·DNA·dNTP ternary complex (0.41 s^{-1}), and the ternary complex after the protein conformational change (0.004 s^{-1}) are significantly different and support the existence of a bona fide protein conformational change step. The rate-limiting protein conformational change was further substantiated by the observation of different reaction amplitudes between pulse-quench and pulse-chase experiments. Additionally, the processivity of Dpo4 was calculated to be 16 at 37 °C from analysis of a processive polymerization experiment. The structural basis for both the protein conformational change and the low processivity of Dpo4 was discussed.

The recently discovered Y-family polymerases are found to bypass a variety of DNA lesions which block DNA synthesis catalyzed by replicative polymerases. All the Y-family polymerases that have thus far been biochemically characterized are devoid of intrinsic proofreading exonuclease activity and are distributive (*1*−*7*). Previous steady-state kinetic studies reveal the Y-family polymerases, when compared to similar studies of replicative polymerases, exhibit fidelity that is 2−3 orders of magnitude lower. This low fidelity is due to the loose polymerase active site and lack of fidelity checking mechanisms as revealed by the high-resolution crystal structure of *Sulfolobus solfataricus* P2 DNA polymerase IV (Dpo4)[1] in a ternary complex with DNA and an incoming nucleotide (*8*). In addition to the signature right-hand shape with palm, finger, and thumb domains found in all structure-known DNA polymerases (*9*−*14*), Dpo4 has an additional fourth domain, designated the "little finger", which is absent in both replicative and repair DNA polymerases. The unique biochemical and structural properties of Y-family polymerases suggest they may utilize different kinetic mechanisms to catalyze DNA synthesis in comparison to replicative and repair polymerases. As established by pre-steady-state kinetic analysis, replicative polymerases such as T7 DNA polymerase utilize an induced-fit mechanism in which polymerase fidelity is a result of conformational coupling, where the energy of nucleotide binding is used to drive a rate-limiting protein conformational change preceding a fast chemistry step (*15*). In contrast, DNA repair polymerases such as rabbit DNA polymerase β (rPolβ) incorporate nucleotides by employing what is known as the rate-limiting transition-state mechanism, in which the free energy difference in chemical transition states between correct and incorrect base pairs dictates polymerase fidelity through a rate-limiting chemistry step (*16*).

Recently, a pre-steady-state kinetic study on yeast polymerase η (yPolη), another Y-family member, with an undamaged DNA substrate was reported (*17*). yPolη, like other replicative polymerases, is shown to utilize the induced-fit mechanism to select and incorporate correct nucleotides during polymerization. However, unlike other DNA polymerases, the protein conformational change, as opposed to the chemistry step, in yPolη is suggested to be the rate-limiting step for the incorporation of mismatched nucleotides.

† This work was supported in part by American Chemical Society Petroleum Research Fund Grant PRF38364-G4, by American Cancer Society Grant IRG-98-278-03, and by TriLink Biotechnologies Research Funding Program to Z.S. K.A.F. was supported by the National Institutes of Health Chemistry and Biology Interface Program at The Ohio State University (Grant T32 GM08512-08).

* To whom correspondence should be addressed. Telephone: (614) 688-3706. Fax: (614) 292-6773. E-mail: suo.3@osu.edu.

‡ Department of Biochemistry and Ohio State Biochemistry Program.

§ Ohio State Biophysics Program, Molecular, Cellular and Developmental Biology Program, and Comprehensive Cancer Center.

[1] Abbreviations: BSA, bovine serum albumin; ddTTP, 2′,3′-dideoxythymidine 5′-triphosphate; dNTP, 3′-deoxynucleoside 5′-triphosphate; Dpo4, *S. solfataricus* P2 DNA polymerase IV; DTT, dithiothreitol; PCNA, proliferating cell nuclear antigen; PP_i, pyrophosphate; rPolβ, rabbit DNA polymerase β; yPolη, yeast DNA polymerase η.

10.1021/bi035746z CCC: $27.50
Published on Web 01/29/2004

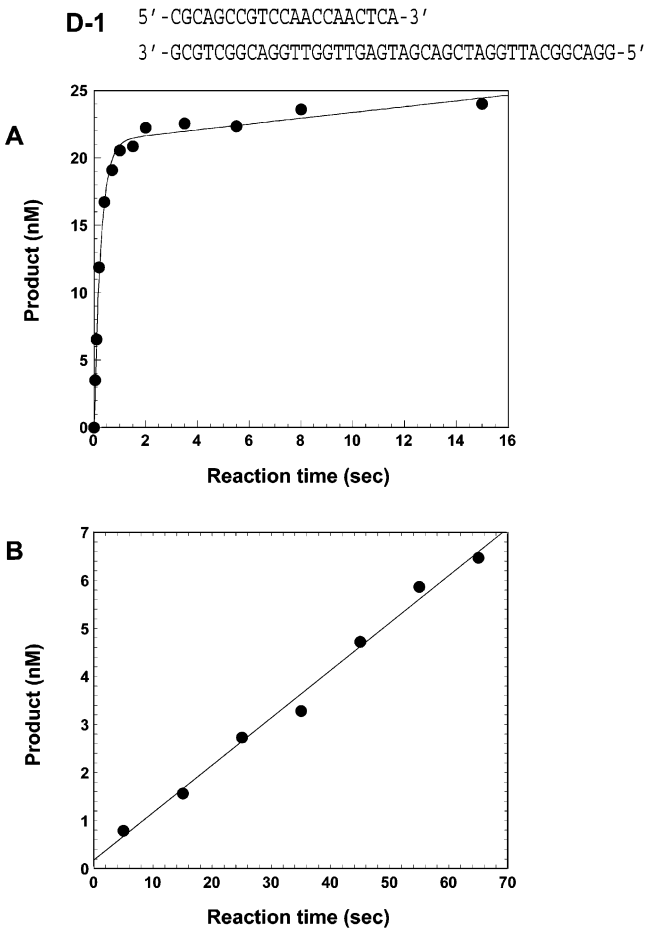

FIGURE 1: Pre-steady-state and steady-state kinetics of incorporation of dTTP into D-1 by Dpo4. (A) A preincubated solution of Dpo4 (30 nM) and D-1 5′-labeled with ^{32}P (120 nM) was mixed with Mg^{2+}·dTTP (0.10 mM) in a rapid chemical quench flow apparatus. The reactions were quenched at various times with 0.37 M EDTA, and products were quantitated by sequencing gel analysis. The data were fit by nonlinear regression to a biphasic curve (eq 1) with rate constants equal to 3.8 ± 0.2 and 0.020 ± 0.002 s^{-1} for the exponential and linear phases, respectively. (B) Incorporation of dTTP into D-1 was independently assessed under steady-state conditions by preincubating Dpo4 (1.2 nM) and D-1 5′-labeled with ^{32}P (250 nM) and then starting the reactions with the addition of Mg^{2+}·dTTP (0.10 mM). Reactions were terminated at various times by the addition of 0.37 M EDTA and quantitated. The data were fit to a straight line (eq 2), and the steady-state rate constant was calculated from the slope of this line divided by the enzyme concentration to give a rate constant equal to 0.07 s^{-1}.

In the preceding paper (*18*), we have implemented pre-steady-state kinetic methods to determine the fidelity of DNA polymerization by Dpo4 (*18*). Here, we employ pre-steady-state kinetic techniques to investigate the kinetic mechanism of DNA polymerization by Dpo4 with an undamaged template. Dpo4, a thermostable archaeal polymerase (*19*), was selected to serve as a model Y-family polymerase because of the ability to obtain milligrams of active enzyme required for pre-steady-state kinetic studies, which can be overexpressed in *Escherichia coli* and purified using common chromatographic methods (*20*). Our kinetic results suggest Dpo4, like yPolη, follows the induced-fit mechanism for nucleotide discrimination. However, the rate-limiting step for the incorporation of an incorrect nucleotide by Dpo4, unlike yPolη, was limited by the chemistry step.

EXPERIMENTAL PROCEDURES

Materials. These chemicals were purchased from the following companies: [α-^{32}P]dTTP and [γ-^{32}P]ATP from Perkin-Elmer Life Sciences (Boston, MA), activated calf thymus DNA from Sigma (St. Louis, MO), dNTPs from Gibco-BRL (Rockville, MD), S_p-dTTPαS and S_p-dGTPαS from Biolog-Life Science Institute (Bremen, Germany), and ddTTP from Trilink Biotechnologies (San Diego, CA). Full-length Dpo4 fused to a C-terminal His_6 tag was overexpressed in *E. coli* as described in ref *18*. The protein was stored in 20 μL aliquots at −80 °C (*18*). The DNA substrate (D-1) listed in Figure 1 was prepared as described previously (*18*).

Pre-Steady-State Kinetic Assays. All experiments using Dpo4, if not specified, were performed in an optimized reaction buffer R containing 50 mM HEPES (pH 7.5 at 37 °C), 5 mM $MgCl_2$, 50 mM NaCl, 0.1 mM EDTA, 5 mM DTT, 10% glycerol, and 0.1 mg/mL BSA. All reactions were carried out at 37 °C using a rapid chemical quench flow apparatus (KinTek) as described previously (*18*).

Measurement of the Rate of DNA Dissociation from the Binary Complex. Direct measurement of the rate of DNA dissociation from the binary complex was obtained by incubating Dpo4 (50 nM) with 5′-radiolabeled D-1 (100 nM) in buffer R and then mixing this solution with trap DNA (1 mg/mL activated calf thymus DNA) for periods of time ranging from 10 s to 20 min. After this variable mixing period, dTTP (100 μM) was consistently added to each reaction mixture for an additional 15 s followed by an EDTA quench. The ensuing reaction products were separated by gel electrophoresis and visualized using a Phosphorimager. The data were subsequently fit to the equation [product] = $A \exp(-kt)$, where k represents the DNA dissociation rate constant and A the product concentration in the absence of the DNA trap.

Pulse-Chase and Pulse-Quench Experiments. Pulse-chase and pulse-quench experiments were performed in buffer R using a rapid chemical quench flow instrument. A preincubated solution containing Dpo4 (30 nM) and unlabeled D-1 (30 nM) loaded into one sample loop was rapidly mixed with buffer containing [α-^{32}P]dTTP (50 μM) from a second sample loop for reaction times ranging from 50 ms to 4.5 s. In the pulse-quench experiment, reactions were immediately quenched with 1 M HCl. In the pulse-chase experiment, reactions were immediately chased with 2.5 mM unlabeled dTTP for 30 s, followed by quenching with 1 M HCl. In both cases, quenched reaction mixtures were treated with chloroform and neutralized with NaOH. Following neutralization, individual samples were quantitated via sequencing gel analysis.

Product Analysis. Reaction products were analyzed by sequencing gel electrophoresis (17% acrylamide, 8 M urea, and 1× TBE running buffer) and quantitated with a Phosphorimager 445 SI (Molecular Dynamics).

Data Analysis. Data were fit by nonlinear regression using KaleidaGraph (Synergy Software). Data from burst experiments were fit to eq 1

$$[\text{product}] = AE_0[1 - \exp(-k_1 t) + k_2 t] \qquad (1)$$

where A is the fraction of active enzyme, E_0 the enzyme

concentration measured spectrophotometrically, k_1 the observed burst rate, and k_2 the observed steady-state rate.

Data from the steady-state kinetic experiments were fit to eq 2

$$[\text{product}] = k_{ss}E_0t + E_0 \quad (2)$$

where k_{ss} is the steady-state rate constant of dNTP incorporation at the initial active enzyme concentration (E_0).

Data from the active site titration were fit to eq 3

$$[\text{E·DNA}] = 0.5(K_d + E_0 + D_0) - 0.5[(K_d + E_0 + D_0)^2 - 4E_0D_0]^{1/2} \quad (3)$$

where K_d represents the equilibrium dissociation constant for DNA substrates, E_0 the active enzyme concentration, and D_0 the DNA concentration.

Data from the single-turnover experiments were fit to eq 4 (single-exponential)

$$[\text{product}] = A[1 - \exp(-k_{obs}t)] \quad (4)$$

where A represents the reaction amplitude and k_{obs} the observed single-turnover rate.

The data from the processive elongation of 21/41-mer to 27/41-mer were modeled using an improved personal computer version of KINSIM provided by C. Frieden (Washington University, St. Louis, MO) (*21*). Final fitting of the data was accomplished by nonlinear regression based on kinetic simulation using an improved personal computer version of FITSIM (*22*).

RESULTS

Burst Kinetics. To determine whether a single-nucleotide incorporation catalyzed by Dpo4 follows the biphasic kinetics as observed in other polymerases (*23*−*28*), a pre-steady-state kinetic analysis for the correct incorporation of dTTP into a DNA substrate D-1 (Figure 1) was performed under conditions where the DNA substrate was in slight molar excess over the enzyme to observe the kinetics of the first and subsequent turnovers of the enzyme (*23*). A preincubated solution of Dpo4 (30 nM) and 5′-[^{32}P]D-1 (120 nM) in one syringe was mixed with dTTP from a second syringe at 37 °C in the optimized reaction buffer R (*18*). The reactions were quenched at time intervals ranging from 5 ms to 15 s. The reaction products were analyzed by sequencing gel electrophoresis and quantitated using a Phosphorimager. The resulting time course of formation of labeled 22/41-mer (Figure 1A) shows the biphasic kinetics: a rapid burst of dTTP incorporation followed by a slower linear phase. The first turnover occurred at a rate of 3.8 ± 0.2 s^{-1} (burst phase), while subsequent turnovers (linear phase) occurred at a much slower rate of 0.020 ± 0.002 s^{-1} (Figure 1A). To confirm the observed linear phase was the bona fide steady-state phase, we conducted an independent steady-state kinetic experiment under conditions where the DNA substrate concentration was approximately 200-fold greater than the enzyme concentration. The observed steady-state rate was 0.07 s^{-1} (Figure 1B) which was similar to the rate observed in the linear phase of the burst experiment (Figure 1A). Thus, the linear phase was indeed the steady-state phase. Like other polymerases (*23*−*28*), the pre-steady-state burst observed in Figure 1A suggested that the burst phase was limited by DNA polymerization in the first turnover and the linear phase was limited by the slow DNA dissociation from the binary complex of the enzyme and DNA (E·DNA). The former could be specifically limited by the protein conformational change step, the chemistry step, or both. The latter was confirmed by the assessment of DNA dissociation from the E·DNA binary complex. A preincubated solution of Dpo4 (50 nM) and 5′-radiolabeled D-1 (100 nM) was mixed with a large excess of activated calf thymus DNA (1 mg/mL) for time intervals varying from 10 s to 20 min. The large excess of calf thymus DNA trapped Dpo4 as it dissociated from the labeled D-1 substrate. The subsequent reaction with dTTP was held constant for 15 s to afford ample time for extension of the available labeled substrate. Reactions were then quenched upon addition of EDTA and mixtures analyzed by gel analysis. The resulting data were fit to a single-exponential equation to yield a rate constant of 0.022 s^{-1} (k_{-1}) which is close to the value of 0.020 s^{-1} observed in the steady-state phase in Figure 1A.

Active Site Titration. Since the catalysis in the first turnover was much faster than the equilibration of the enzyme and DNA (E + DNA = E·DNA), a titration of the enzyme active site with DNA can be used to measure the equilibrium dissociation constant (K_d) of the E·DNA binary complex by examining the DNA concentration dependence of the first-turnover amplitude (*23*). A preincubated solution of Dpo4 (22 nM, as determined by UV absorbance measurements), Mg^{2+}, and an increasing concentration of D-1 5′-labeled with ^{32}P was rapidly mixed with dTTP and Mg^{2+}. Reactions were quenched with EDTA after 1.2 s which allowed adequate time for the reaction to reach the maximum first-turnover amplitude with a negligible contribution of multiple turnovers. The products were analyzed by sequencing gel electrophoresis. The experiments were performed in triplicate, and the mean product concentration was plotted against the DNA concentration. The solid line (Figure 2) was a fit of the data to a quadratic equation (see Experimental Procedures) which gave a K_d value for the active complex of Dpo4 and DNA 21/41-mer of 10.6 ± 1.3 nM, and an enzyme amplitude of 19.4 ± 0.5 nM or 88% of the protein concentration measured spectrophotometrically at 280 nm (*18*). Thus, the enzyme is not 100% active, and the enzyme concentrations for the following experiments were corrected for the amount of active enzyme. On the basis of the DNA dissociation rate of 0.02 s^{-1} (see above), the apparent second-order binding rate constant of the Dpo4·21/41-mer complex was thus calculated ($k_{on} = k_{off}/K_d = 1.9 \times 10^6$ M^{-1} s^{-1}). This indicated the rate of binding of DNA to Dpo4 was below the diffusion limit. A similar phenomenon has been observed previously for the binding of DNA to T7 DNA polymerase (1.12×10^7 M^{-1} s^{-1}) (*23*).

Rates of Association and Dissociation of the Incoming Nucleotide. In the preceding paper (*18*), the ground-state binding affinity of dTTP (K_d) was measured through the dTTP concentration dependence of the single-turnover rate, yielding the maximum dTTP incorporation rate (k_p) of 9.4 ± 0.3 s^{-1}, and a K_d of 230 ± 17 μM for the binding of dTTP. Since the active site of Dpo4 is loose and relatively accessible to solvent as revealed by the crystal structure of Dpo4 (*8*), we assume the upper limit of the association rate constant of dTTP (k_{on}) is close to the diffusion limit of 1.0

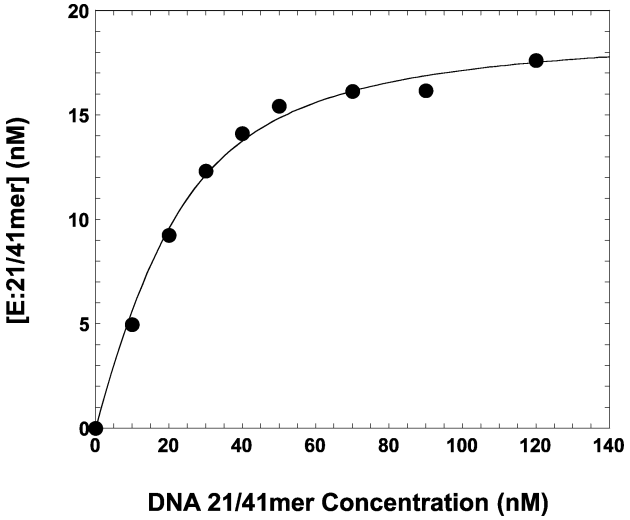

FIGURE 2: Active site titration of Dpo4 with D-1. A solution of Dpo4 (22 nM as determined by UV absorbance measurements) was preincubated with increasing concentrations of D-1 5′-labeled with ^{32}P and subsequently mixed with a solution containing Mg^{2+}·dTTP (0.10 mM) in a rapid chemical quench flow apparatus. The reactions were quenched after 1.2 s, and the products were analyzed by sequencing gel electrophoresis. The burst amplitude was then plotted as a function of substrate concentration, and the data were fit to the quadratic equation (eq 3) which gave a K_d for the Dpo4−D-1 complex of 10.6 ± 1.3 nM and an enzyme amplitude of 19.4 ± 0.5 nM.

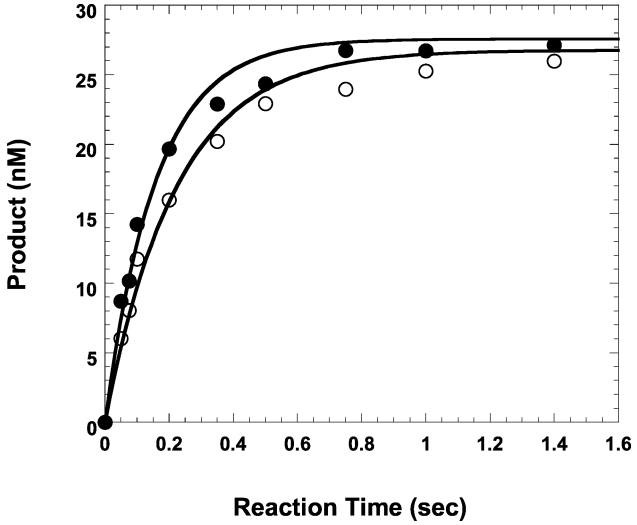

FIGURE 3: S_p-dTTP(αS) elemental effect on the rate of correct nucleotide incorporation. A preincubated solution of Dpo4 (120 nM) and D-1 5′-labeled with ^{32}P (30 nM) was mixed with either 0.10 mM Mg^{2+}·dTTP (●) or Mg^{2+}·S_p-dTTPαS (○) in parallel time courses. The products were quantitated, and the data were fit by nonlinear regression to the single-exponential equation (eq 4), yielding k_{obs} values of 6.27 ± 0.38 and 4.49 ± 0.30 s^{-1} for dTTP and S_p-dTTPαS, respectively. The elemental effect of 1.4 was calculated from the ratio of the k_{obs} values for correct nucleotide incorporation into D-1.

Scheme 1

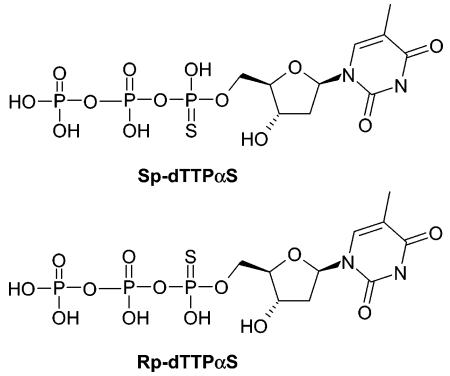

× 10^8 M^{-1} s^{-1}. The upper limit of the dissociation rate constant for dissociation of dTTP from the E·DNA·dNTP complex was thereby estimated ($k_{off} = k_{on}K_d = 23\,000\ s^{-1}$). This dNTP dissociation rate is too fast to be measured by current rapid chemical quench and stopped flow techniques.

Elemental Effect of the Incorporation of a Matched Incoming Nucleotide. The maximum incorporation rate, k_p, can be a direct measure of the chemistry step of phosphodiester bond formation, the protein conformational change step preceding the chemistry step, or both. To distinguish between these three possibilities, the effect of an incoming nucleotide analogue, characterized by a substitution of the α-phosphate with a phosphothioate group (Scheme 1), on k_{obs}, the observed incorporation rate, was assayed. This approach was based on the observations that a rate-limiting chemical step involving the making or breaking of a phosphate bond shows a phosphothioate elemental effect (*29*, *30*). A preincubated solution of Dpo4 (120 nM) and D-1 5′-labeled with ^{32}P (30 nM) was reacted with either dTTP (100 μM) or S_p-dTTPαS (100 μM, >95% pure) in buffer R. The S_p isomer (Scheme 1), rather than the R_p isomer of dTTPαS, was used due to the stereoselectivity of polymerases in the presence of Mg^{2+} as observed with rPolβ (*31*). The reactions were quenched at various times. The data were fit into a single-exponential equation (eq 4) with k_{obs} values of 6.27 ± 0.38 and 4.49 ± 0.30 s^{-1} for dTTP and S_p-dTTPαS, respectively (Figure 3). Therefore, the elemental effect of the matched dTTP incorporation was 1.4. On the basis of modeling studies of the hydrolysis of phosphate diesters (*29*), an elemental effect of 4−11 has generally been taken as evidence of a rate-limiting chemistry step during DNA synthesis catalyzed by a polymerase (*17*). This suggested the chemistry step was not rate-limiting for the incorporation of correct nucleotides by Dpo4 in the burst phase. This conclusion was consistent with the experimental results shown below.

Elemental Effect of the Incorporation of a Mismatched Incoming Nucleotide. To probe whether the chemistry step, the protein conformational change step, or both were rate-limiting during incorrect nucleotide incorporation, an analogous elemental effect study was performed with the incorporation of mismatched incoming dGTP into D-1. A preincubated solution of Dpo4 (120 nM) and D-1 5′-labeled with ^{32}P (30 nM) was reacted with either dGTP (100 μM) or S_p-dGTPαS (100 μM, >95% pure) in buffer R, and the products were analyzed and quantitated as described above. The observed single-turnover rates (k_{obs}) were 0.0021 ± 0.0001 and 0.00037 ± 0.00002 s^{-1} for dGTP and S_p-dGTPαS, respectively (Figure 4). The elemental effect of incorporation of dGTP into D-1 was calculated to be 5.8, which suggested the chemistry step limits the rate of incorrect nucleotide incorporation (*29*). However, additional evidence is required to confirm this observation.

Notably, we performed experiments assessing a possible elemental effect for both correct and incorrect nucleotide incorporations at subsaturating nucleotide concentrations based on our results from nucleotide binding (*18*). However,

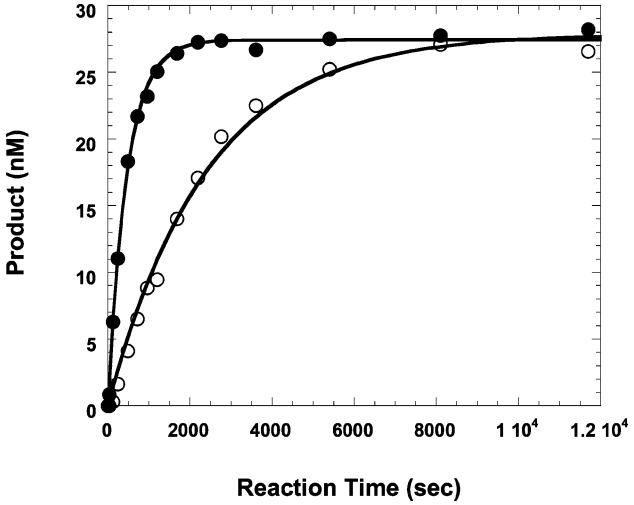

FIGURE 4: S_p-dGTP(αS) elemental effect on the rate of incorrect nucleotide incorporation. A preincubated solution of Dpo4 (120 nM) and D-1 5′-labeled with ^{32}P (30 nM) was mixed with either 0.10 mM Mg^{2+}·dGTP (●) or Mg^{2+}·S_p-dGTPαS (○) in parallel time courses. The products were quantitated, and the data were fit by nonlinear regression to the single-exponential equation (eq 4), yielding k_{obs} values of 0.0021 ± 0.0001 and 0.00037 ± 0.00002 s^{-1} for dGTP and S_p-dGTPαS, respectively. The elemental effect of 5.8 was calculated from the ratio of the k_{obs} values for incorrect nucleotide incorporation into D-1.

since the difference between the maximum incorporation rate k_p and the observed k_{obs} at a subsaturating dNTP concentration equals [dNTP]/(K_d + [dNTP]), the value of the elemental effect derived from the k_p ratio should be identical or similar to the elemental effect derived from the k_{obs} ratio if the K_d values of dNTP and S_p-dNTPαS are equal or close. Due to the lack of interactions between Dpo4 and the nucleotide at the polymerase active site revealed by ternary crystal structures of Dpo4 (*8*), there will be essentially no difference in the binding of dNTP and its α-thio analogue and the K_d difference will be minimal at best. Structural analyses of other polymerase active sites, like DNA polymerase *β*, also suggest a minimal difference between the ground-state binding affinity of dNTP and its analogue dNTPαS (*31*).Therefore, the subsaturating concentrations of nucleotides dNTP and dNTPαS used in our studies should not affect the value of the elemental effect and the overall conclusion.

Processive Polymerization. The processivity of Dpo4 was investigated by including three dNTPs in the reaction mixture, thus permitting the elongation of D-1, a 21/41-mer DNA substrate, to a 27/41-mer. The experiment was performed under conditions where D-1 was in molar excess over Dpo4 to ensure the measured kinetics of sequential elongation steps were a function of single-enzyme binding events. A preincubated solution of Dpo4 (35 nM) and D-1 5′-radiolabeled with ^{32}P (100 nM) was mixed with dTTP, dCTP, and dGTP (1.2 mM each) in reaction buffer R with Mg^{2+} compensation (see above) for reaction times ranging from several milliseconds to 2.5 s prior to being quenched with EDTA and subsequently analyzed by a gel assay. The time courses of product formation and substrate disappearance were fit by nonlinear regression using computer simulation programs Kinsim (*21*) and Fitsim (*22*) and a mechanism consisting of a series of six single-nucleotide incorporations and DNA dissociations (Figure 5). The rate constants of formation of intermediates were as follows: 2.3

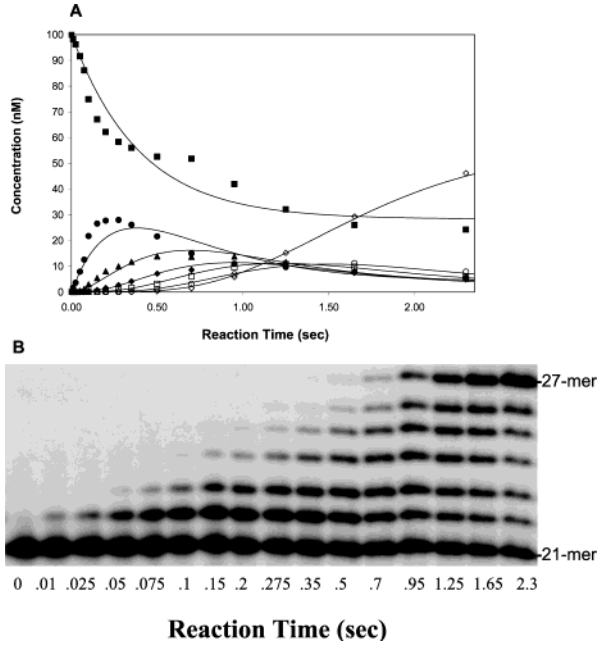

FIGURE 5: Processive polymerization by Dpo4. (A) A preincubated solution of Dpo4 (35 nM) and D-1 5′-labeled with ^{32}P (100 nM) was rapidly mixed with dTTP, dCTP, and dGTP (1.2 mM each) in the reaction buffer containing Mg^{2+}. The reactions were quenched at various times with 0.37 M EDTA and the mixtures analyzed by sequencing gel analysis. The amount of remaining substrate 21-mer (■) and each product formed [22-mer (●), 23-mer (▲), 24-mer (◆), 25-mer (□), 26-mer (○), and 27-mer (◇)] was plotted as a function of the reaction time. The solid lines represent best fits obtained from computer simulation using a mechanism consisting of a series of six single-nucleotide incorporations at 2.3 ± 0.1 (22-mer), 2.9 ± 0.2 (23-mer), 3.5 ± 0.4 (24-mer), 4.3 ± 0.6 (25-mer), 3.9 ± 0.6 (26-mer), and 3.4 ± 0.4 s^{-1} (27-mer), respectively, and DNA dissociations at 0.26 ± 0.05 (21/41-mer), 0.18 ± 0.11 (22/41-mer), 0.19 ± 0.12 (23/41-mer), 0.18 ± 0.16 (24/41-mer), 0.18 ± 0.18 (25/41-mer), 0.15 ± 0.11 (26/41-mer), and 0.20 ± 0.09 s^{-1} (27/41-mer). (B) Image of the results from the processivity experiment after analysis by sequencing gel electrophoresis showing the progress of the six single-nucleotide incorporations at various reaction times.

± 0.1 s^{-1} for 22-mer, 2.9 ± 0.2 s^{-1} for 23-mer, 3.5 ± 0.4 s^{-1} for 24-mer, 4.3 ± 0.6 s^{-1} for 25-mer, 3.9 ± 0.6 s^{-1} for 26-mer, and 3.4 ± 0.4 s^{-1} for 27-mer. This simulation also provided DNA dissociation rates: 0.26 ± 0.05 s^{-1} for 21/41-mer, 0.18 ± 0.11 s^{-1} for 22/41-mer, 0.19 ± 0.12 s^{-1} for 23/41-mer, 0.18 ± 0.16 s^{-1} for 24/41-mer, 0.18 ± 0.18 s^{-1} for 25/41-mer, 0.15 ± 0.11 s^{-1} for 26/41-mer, and 0.20 ± 0.09 s^{-1} for 27/41-mer. These dissociation rates in the range of 0.15−0.26 s^{-1} were much higher than the E·DNA dissociation rate of 0.02 s^{-1} (Figure 1). If DNA dissociated at a rate of 0.02 s^{-1}, each of the intermediates shown in Figure 5 should have returned to the baseline as in the case of T7 DNA polymerase (*23*). However, the intermediates accumulated in the range of 5−10 nM which suggested that DNA dissociated at a faster rate from a yet unidentified intermediate state formed after the binding of dNTP to the E·DNA complex. This intermediate could be the initial binding E·DNA·dNTP complex, the E′·DNA·dNTP complex after a putative protein conformational change, or the E′·DNA·PP_i complex after the chemistry step.

Measurement of the DNA Dissociation Rate of the E·DNA·dNTP Complex. DNA can either dissociate from the ternary complex (E·DNA·dNTP) or be converted to product after

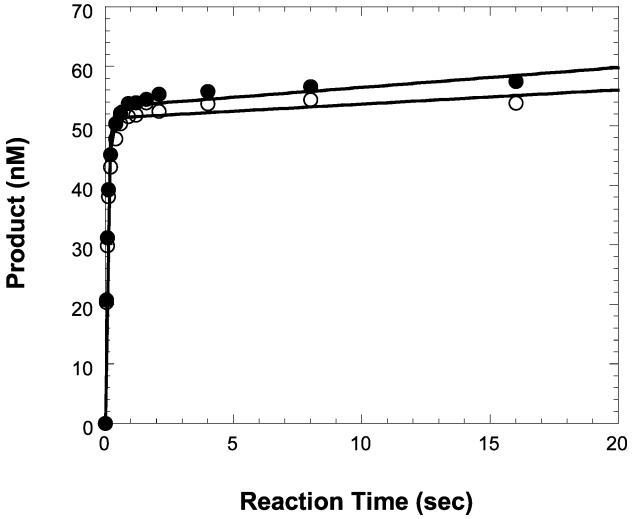

FIGURE 6: Measurement of the DNA dissociation rate of the E·DNA·dNTP complex. A preincubated solution of Dpo4 (55 nM) and D-1 5′-labeled with ^{32}P (60 nM) was mixed with Mg^{2+}·S_p-dTTPαS (1.2 mM) in the absence (●) or presence (○) of unlabeled trap D-1 (2.5 μM). The rate of incorporation in the both experiments was 11.0 s^{-1}; however, the burst amplitudes were 53.1 ± 0.6 and 51.2 ± 0.7 nM in the absence and presence of DNA trap, respectively. This reduction in amplitude (3.6%) in the presence of the trap suggests a rate of DNA dissociation from this ternary complex of 0.41 s^{-1}.

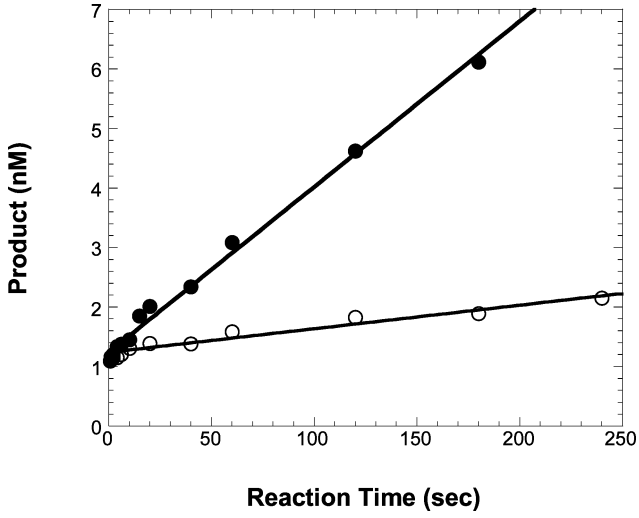

FIGURE 7: Measurement of the DNA dissociation rate of the E′·DNA·dNTP complex. A preincubated solution of Dpo4 (1.2 nM) and D-1 5′-labeled with ^{32}P (200 nM) was mixed with Mg^{2+}·ddTTP (1.2 mM) in the absence (●) or presence (○) of the next correct nucleotide, dCTP (1.2 mM). The steady-state rate constant in the absence of dCTP was 0.028 ± 0.001 s^{-1} and corresponds to the rate of dissociation of DNA from the E·DNA binary complex, while the rate constant in the presence of dCTP was 0.0040 ± 0.0003 s^{-1} and corresponds to the rate of dissociation of DNA from the E′·DNA·dNTP ternary complex.

the putative protein conformational change and chemistry steps. To measure the DNA dissociation rate (k_{off}) of the E·DNA·dNTP complex, the nucleotide analogue S_p-dTTPαS, rather than dTTP, was used in this assay to procure a slightly larger kinetic partitioning due to the slower rate of incorporation of S_p-dTTPαS relative to dTTP (Figure 3). A large molar excess of unlabeled D-1 was used to trap any dissociated enzyme molecules which were bound by radiolabeled DNA substrate molecules. The experiment was conducted by reacting a preincubated solution of Dpo4 (55 nM) and 5′-radiolabeled D-1 (60 nM) with S_p-dTTPαS (1.2 mM) alone or with S_p-dTTPαS (1.2 mM) and unlabeled D-1 (2.5 μM). Incorporation of S_p-dTTPαS occurred at a rate of 11.0 s^{-1} (k_{obs}) in both time courses, but the amplitudes of the burst were 53.1 ± 0.6 and 51.2 ± 0.7 nM in the absence and presence of the DNA trap, respectively (Figure 6). Since the relative amplitude (51.2/53.1) is equal to $k_{obs}/(k_{obs} + k_{off})$, the dissociation rate k_{off} of the E·DNA·dNTP complex was estimated to be 0.41 s^{-1}. This rate was similar to the rates observed in Figure 5, indicating the low processivity of Dpo4 was due to fast DNA dissociation from the E·DNA·dNTP ternary complex. Similar results have been observed with HIV-1 reverse transcriptase (*26*).

Measurement of the Dissociation Rates of the E′·DNA·dNTP Complex. Steady-state kinetic experiments were used to measure the rate of dissociation of DNA from a E′·DNA·dNTP complex that could not undergo the chemical step due to the presence of ddTTP that, once incorporated, does not have the required hydroxyl group at the 3′-end of the primer strand for a subsequent extension reaction. The experiments were conducted by reacting a preincubated solution of Dpo4 (1.2 nM) and 5′-radiolabeled D-1 (200 nM) with ddTTP (1.2 mM) alone or with ddTTP (1.2 mM) and the next correct nucleotide dCTP (1.2 mM). The steady-state rate in the presence of ddTTP alone (0.028 ± 0.001 s^{-1}) (Figure 7) was a direct measure of the rate of dissociation of DNA from the E·DNA product complex. This rate was close to the steady-state rate measured in Figure 1. In the presence of ddTTP and dCTP, an extremely slow off rate of 0.0040 ± 0.0003 s^{-1} was observed from the dissociation of the E′·DNA·dNTP complex (Figure 7). Similar results were observed previously in HIV-1 reverse transcriptase (*26*). These results suggested the binding of the next correct nucleotide inhibits the dissociation of DNA from the E′·DNA·dNTP complex. More importantly, the slow dissociation of DNA from the E′·DNA·dNTP complex provided kinetic evidence for the existence of the protein conformational change prior to the chemistry step.

Pulse-Chase and Pulse-Quench Experiments. Pulse-chase and pulse-quench experiments were conducted to seek additional but independent evidence for the existence of a slow conformational change step that would precede the chemistry step in the incorporation of a matched nucleotide by Dpo4. These experiments were carried out by comparing two separate time courses. In each case, a preincubated solution of Dpo4 (30 nM) and unlabeled D-1 (30 nM) was mixed with [α-^{32}P]dTTP (50 μM) for various time intervals in a rapid chemical quench flow instrument. In the first experiment, reactions were quenched by the addition of 1 M HCl, while in the second experiment, each reaction mixture was chased with unlabeled dTTP (2.5 mM) for an additional 30 s, followed by an acid quench (1 M HCl). The reaction mixtures were denatured by the addition of chloroform and neutralized with 1 M NaOH prior to analysis by sequencing gel electrophoresis. In the pulse-quench reactions, 1 M HCl quenched all the enzyme-bound species. In the chased reaction mixtures, the enzyme-bound complex was allowed to partition between both the reverse and forward directions, and a stable bound complex of Dpo4, DNA, and [α-^{32}P]dTTP, if any, would be chased by the large amount of cold dTTP in the forward direction to form an excess of radiolabeled product. Comparison of the kinetics of these

Scheme 2

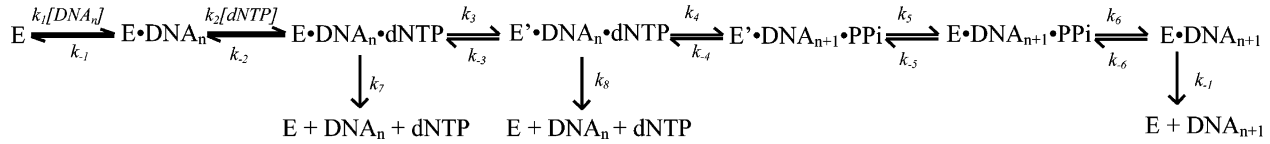

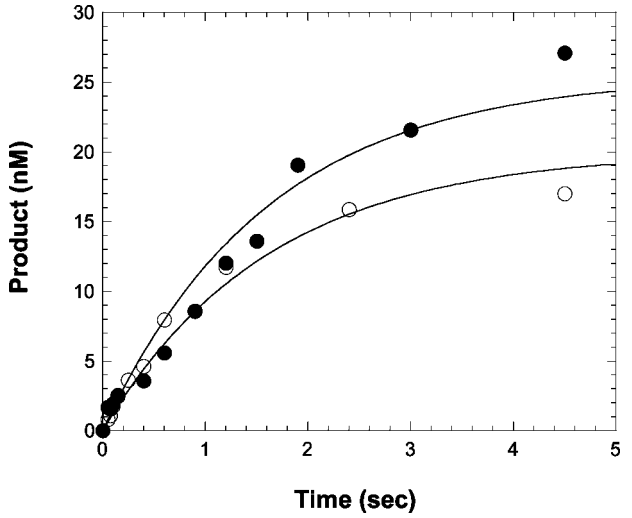

FIGURE 8: Pulse-chase and pulse-quench experiment. A preincubated solution of Dpo4 (30 nM) and unlabeled D-1 (30 nM) was mixed with [α-^{32}P]dTTP (50 μM) for time intervals ranging from 0.05 to 4.5 s. The reactions in these two experiments were either quenched directly with 1 M HCl (pulse quench) or chased with 2.5 mM unlabeled dTTP (pulse chase) for 30 s, followed by HCl quenching. Both experiments were fit to the single-exponential equation (eq 4), yielding amplitudes of 20 ± 0.6 and 25.5 ± 1.0 nM and observed rates of 0.62 ± 0.17 and 0.62 ± 0.24 s^{-1} for the pulse-quench (○) and pulse-chase (●) experiments, respectively.

experiments provided direct evidence for the existence of an enzyme-bound complex preceding the chemical step (*23*, *32*). The pulse-quench data were fit to a single-exponential equation to yield an amplitude of 20.0 ± 0.6 nM and a rate constant of 0.62 ± 0.17 s^{-1}. The chased data were also fit to a single-exponential equation with an amplitude of 25.5 ± 1.0 nM and a corresponding rate of 0.62 ± 0.24 s^{-1} (Figure 8). The incorporation rates of [α-^{32}P]dTTP (50 μM) for the pulse-chase and pulse-quench experiments were lower than expected (~2 s^{-1}), and it was due to experimental error. The obvious difference in amplitudes (5.5 nM) between the two sets of experiments was reproducible and demonstrated the formation of an intermediate complex prior to the chemical step (*23*, *32*). Theoretically, this intermediate complex could be either the E·DNA, E·DNA·dNTP, or E′·DNA·dNTP complex. However, we know that this complex cannot be the E·DNA binary complex since such an intermediate would bind cold dTTP under the pulse-chase conditions and be removed from observation. This would result in identical curves in each of the two sets of experiments. Likewise, this intermediate species was not the E·DNA·dNTP ternary complex since the difference in amplitudes (~20%) would require that the complex partitioned between formation of product (amplitude = 80%, 2 s^{-1}) and release of dTTP to form the E·DNA complex (~0.09 s^{-1}) and form E, DNA, and dTTP (0.41 s^{-1}) (*32*). The off rate of dTTP from the E·DNA·dNTP complex is much slower than the estimated dissociation rate of dTTP (23 000 s^{-1}) based on its ground-state binding affinity (see above).

Table 1: Estimated Kinetic Constants of Dpo4

parameter	value	parameter	value
k_1	1.9 μM^{-1} s^{-1}	$K_{d,dNTP}$	230 μM
k_{-1}	0.02 s^{-1}	k_3	9.4 s^{-1}
$K_{d,DNA}$	10.6 nM	k_7	0.41 s^{-1}
k_2	100 μM^{-1} s^{-1}	k_8	0.004 s^{-1}
k_{-2}	23000 s^{-1}		

The high off rate of dNTP from the E·DNA·dNTP complex has also been estimated with T7 DNA polymerase (≥1000 s^{-1}) (*23*) and the Klenow fragment of *E. coli* DNA polymerase I (≥250 s^{-1}) (*33*). Therefore, this intermediate species was most likely the E′·DNA·dNTP ternary complex.

DISCUSSION

In this paper, we have established the elementary steps of nucleotide incorporation into undamaged DNA catalyzed by Dpo4. On the basis of our pre-steady-state kinetic results, we propose a kinetic mechanism for DNA polymerization by Dpo4 shown in Scheme 2. In Scheme 2, E, DNA$_n$, dNTP, and PP$_i$ represent Dpo4, D-1, dTTP, and pyrophosphate, respectively. The estimated kinetic constants are listed in Table 1. On the basis of the previous findings that free DNA polymerases, such as *E. coli* polymerase I (*34*) and T7 DNA polymerase (*23*), do not specifically bind a nucleotide prior to the binding of DNA, we propose Dpo4 first binds DNA followed by dNTP, to form the E·DNA·dNTP ternary complex. The pre-steady-state time course of single-dTTP incorporation revealed biphasic kinetics (Figure 1). The burst of product formation in the first turnover was limited by nucleotide incorporation, while the slow steady-state phase of the subsequent turnovers was limited by the dissociation of the DNA product from the enzyme. The steady-state turnover rate was further measured and confirmed by two independent steady-state kinetic experiments with dTTP (Figure 1B) and ddTTP (Figure 7), and a third experiment involving the direct measurement of the dissociation rate of the E·DNA binary complex (see Experimental Procedures). The rate-limiting step in the first turnover was determined to be the first protein conformational change after the initial collision of dNTP with the E·DNA binary complex (E·DNA·dNTP ↔ E′·DNA·dNTP). We have observed three lines of evidence supporting such a protein conformational change. (i) The small elemental effect of 1.4 for the incorporations of dTTP versus S_p-dTTPαS suggested the chemistry step was not rate-limiting based on the previous studies of the elemental effect (4−11) observed in the hydrolysis of pyrophosphate (*29*). This approach has been used to establish the rate-limiting step in the nucleotide incorporation catalyzed by other polymerases (*17*, *23*, *35*, *36*). Thus, the potential rate-limiting step must be a step preceding the chemistry step (step 4 in Scheme 2). Since the initial binding of dNTP (step 2) is a fast equilibrium step, the only candidate was the intermediate step between steps 2 and 4 (Scheme 2) which was therefore suggested to be the protein conformational

change. (ii) In the presence of ddTTP and the next correct nucleotide, dCTP, we observed an extremely slow rate of dissociation (0.004 s^{-1}) of DNA from a ternary complex which could not undergo the chemistry step for the incorporation of dCTP due to the lack of a 3′-hydroxyl group on the primer strand after the incorporation of ddTTP (Figure 7). Since the dissociations of the E·DNA (0.02−0.07 s^{-1}) and E·DNA·dNTP (0.41 s^{-1}) complexes were much faster, the tight binding ternary complex observed in the presence of ddTTP and dCTP was thus deduced to be the E′·DNA·dNTP complex. After the initial binding of dNTP to form the loose E·DNA·dNTP complex, the enzyme undergoes an isomerization to tighten the binding of both DNA and dNTP at the active site. The fast dissociation of the E·DNA·dNTP complex was observed in the processive polymerization experiment shown in Figure 5, and the rate was measured directly by following kinetic partitioning in the incorporation of S_p-dTTPαS in the presence of an unlabeled DNA trap (Figure 6). (iii) The reaction amplitude difference between the pulse-chase (25.5 nM) and pulse-quench (20.0 nM) experiments clearly indicated the existence of the E′·DNA·[α-^{32}P]dTTP complex which accumulated but was chased forward by a large excess of cold dTTP (Figure 8). Such an amplitude difference has been observed in *E. coli* DNA polymerase I (*32*), T7 DNA polymerase (*23*), and yPolη (*17*). In addition, ∼5.5 nM of the pool of Dpo4 was in the E′·DNA·[α-^{32}P]dTTP complex which did not yield products under pulse-quench conditions, but was chased to products by a large excess of cold dTTP under the pulse-chase conditions. For the E′·DNA·[α-^{32}P]dTTP complex to accumulate, it is necessary to have a step after the chemistry step to serve as a kinetic "roadblock" (*32*). If PP_i dissociated rapidly after the chemistry step, the E′·DNA·[α-^{32}P]dTTP complex would not accumulate. A slow conformational change (E′·DNA_{n+1}·PP_i ↔ E·DNA_{n+1}·PP_i) is thus included in Scheme 2. However, further evidence is required to confirm the presence of this step. Additional experiments, particularly those that investigate the reverse elementary steps, are needed to measure the remaining microscopic rate constants in Scheme 2.

Induced-Fit Mechanism of Nucleotide Incorporation. Scheme 2 shows Dpo4, like yPolη (*17*) and other polymerases (*23*−*28*), uses the induced-fit mechanism to select correct incoming nucleotides. The fidelity of Dpo4 was contributed primarily by the protein conformational change preceding the chemistry step [see the preceding paper (*18*)]. At present, the contributions of individual amino acid residues and domains of Dpo4 to the protein conformational change have not been explicitly defined due to the lack of structural information regarding the binary complex of a Y-family polymerase and DNA. However, a superimposition of the conserved palm domains of Dpo4 in its ternary complex (*8*) and yPolη alone (*37*) reveals a protein conformational change: the inward rotation of the finger and little finger domains of Dpo4 toward DNA by ∼48° (*38*). The superimposition of the structure of yPolη alone (*37*) with the recently determined structure of Dpo4 in the presence of DNA (containing a *cis-syn* T−T dimer) and a correct incoming nucleotide also suggests a large conformational change for Dpo4: 16°, 16°, and 45° for the finger, thumb, and little finger domains, respectively (*39*). The large swing of the finger domain between the "open" conformation of the E·DNA complex and the "closed" conformation of the E′·DNA·dNTP complex has been observed in other polymerases such as T7 DNA polymerase (*13*), HIV-1 reverse transcriptase (*12*), *Thermus aquaticus* DNA polymerase I (*9*), and DNA polymerase β (*10*). In contrast, the structure of Dbh, a homologue of Dpo4 from the P1 strain of S. *solfataricus*, in the absence of both DNA and an incoming dNTP (*40*, *41*), shows this Y-family polymerase appears to be in the closed conformation. Results from the overlay of this structure with the Dpo4′·DNA·dNTP ternary structure show no obvious structural change which appears to support the conclusion reached by these authors that the "induced-fit" mechanism does not apply to Y-family polymerases (*41*). However, this conclusion contradicts our kinetic observations for Dpo4 and the previously published kinetic results of yPolη which suggest a rate-limiting protein conformational change during correct nucleotide incorporation (*17*). We speculate that the closed conformation observed in the Dbh crystal structure (*40*, *41*) is probably a result of crystal packing and does not reflect the inherent protein conformation in solution. This speculation is somewhat supported by the unusual fact that DNA and a correct incoming nucleotide are required in the crystallization buffer for growth of the crystals of the full-length Dbh alone (*40*). It would be extremely interesting to see the NMR structures of Dbh and Dpo4 in solution. Alternatively, the protein conformational change for a Y-family polymerase could occur exclusively in the unique little finger domain, rather than the finger domain as observed in replicative and repair DNA polymerases. This possibility is unlikely considering that the little finger domain of Dpo4 is not an essential component of the active site (*42*). However, it is possible that a large swing of the little finger domain leads to minor adjustment of the positions of the DNA, nucleotide, and active site residues of Dpo4. Since the E′·DNA·dNTP ternary complex of Dpo4 has been determined (*8*), the structural insight into the first conformational change in Scheme 2 will be clear once the structure of the Dpo4·DNA binary complex is available. On the basis of the kinetic results of the two Y-family polymerases Dpo4 and yPolη (*17*), we further speculate that the induced-fit mechanism may apply to all Y-family DNA polymerases.

Processivity of Dpo4. On the basis of the rate constants derived from the processive DNA synthesis experiment (Figure 5), the average DNA dissociation and product formation rates during processive polymerization were calculated to be 0.21 and 3.3 s^{-1}, respectively. Processivity, defined as the ratio of the polymerization rate divided by the DNA dissociation rate, was calculated to be 16 at 37 °C for Dpo4. This was slightly higher than the processivity of yPolη (5.2) (*17*), and was similar to the previously estimated processivity of Dpo4 with the same DNA/enzyme ratio (*20*). The processivity of Dpo4 and yPolη is much lower than the processivity of replicative polymerases such as T7 DNA polymerase (1500) and human mitochondrial DNA polymerase γ (2250) (*43*). The low processivity of the Y-family polymerases combined with their low fidelity is consistent with their role in the bypass of DNA lesions. In theory, the Y-family polymerases are envisioned to dissociate from DNA shortly after traversing a damaged site, allowing a high-fidelity replicative polymerase to "reassociate" with the DNA and continue processive synthesis. Since *S. solfataricus* is

an aerobic crenarchaeon that metabolizes sulfur and grows optimally at 80 °C and pH 2−4 (*19*), its genome is more likely to undergo depurination and depyrimidination reactions. The resulting abasic lesions are probably bypassed by Dpo4, thus suggesting an adaptive feature provided by this enzyme for the survival of *S. solfataricus* under such harsh conditions (*20*). We are currently studying the fidelity of lesion bypass by Dpo4 using pre-steady-state kinetics.

The high processivity of replicative polymerases is due to the function of the processivity factors associated with these polymerases, e.g., *E. coli* thioredoxin for T7 DNA polymerase, the small subunit for human mitochondrial DNA polymerase γ, and eukaryotic proliferating cell nuclear antigen (PCNA) for polymerases δ and ϵ (*44*). The processivity of several Y-family polymerases, including Dbh (*45*) and *E. coli* DNA polymerase IV (*46*), is greatly increased in the presence of cofactors, but the processivity of human DNA polymerase κ is not affected (*47*). Recently, a heterotrimer of three PCNA homologues (PCNA1, -2, and -3) from *S. solfataricus* P2 was found to dramatically increase the processivity of *S. solfataricus* DNA polymerase B1 (*48*, *49*). It will be interesting to test the effect of the *S. solfataricus* PCNA heterotrimer on the processivity of Dpo4. If the processivity of Dpo4 is increased greatly, the protein complex could be used in the error-prone polymerase chain reactions (PCRs) to engineer random mutations since the fidelity of Dpo4 is low (*18*, *20*, *50*). The biological implication of the potential interactions between Dpo4 and the PCNA heterotrimer requires additional studies.

DNA Binding Affinity. The affinity of Dpo4 for a synthetic DNA substrate, D-1, was measured to be 10.6 nM using the active site titration assay (Figure 2). This indicates Dpo4 binds DNA with the same affinity as replicative polymerases such as T7 DNA polymerase (18 nM) (*23*), human mitochondrial DNA polymerase γ (9.9 nM) (*43*), HIV-1 reverse transcriptase (4.7 nM) (*26*), and the repair enzyme *E. coli* DNA polymerase I (5 nM) (*36*). This is not surprising since, overall, the DNA binding pocket in polymerases is quite large and the interactions between DNA and these polymerases are quite intense. The little finger domain and the tether linking the thumb and little finger domains of Dpo4, which are absent in replicative polymerases, wrap around DNA, acting like a small clamp (*8*). These unusual structural features compensate for the abnormally small thumb and finger domains of Dpo4, increasing the DNA binding affinity. This is confirmed by the significantly lower processivity of a truncated Dpo4 mutant lacking the little finger domain when compared to the processivity of wild-type Dpo4 (*8*).

The faster dissociation of the E·DNA·dNTP ternary complex (0.41 s^{-1}) compared to that of the E·DNA binary complex (0.02−0.07 s^{-1}) is very intriguing. Similar results have been observed for HIV-1 RT (*26*). This phenomenon suggests that correct dNTP binding causes an increase in the rate of DNA dissociation from the enzyme. The structural implication of faster DNA dissociation is not clear. We speculate that the binding of a correct nucleotide may disrupt various specific interactions between DNA and the enzyme such as hydrogen bonding and van der Waals contacts. However, the faster protein conformational change, E·DNA·dNTP ↔ E′·DNA·dNTP (9.4 s^{-1}), in the presence of a correct incoming nucleotide, will limit the effect that the dissociation of DNA from the E·DNA·dNTP complex has on substrate elongation due to favorable kinetic partitioning. More importantly, this protein conformational change step leads to the formation of a tighter binding state, E′·DNA·dNTP, which dissociates at a rate of 0.004 s^{-1} (Figure 7). Thus, the protein conformational change results in a tighter binding of DNA to Dpo4. Similar results have been observed in HIV-1 reverse transcriptase (*26*).

Rate-Limiting Step in the Incorporation of a Mismatched Nucleotide. The elemental effect for the incorporations of a mismatched dGTP and S_p-dGTPαS was measured to be 5.8 (Figure 4), suggesting the chemistry step is rate-limiting for the incorporation of incorrect nucleotides. This conclusion is solely based on the elemental effect of 4−11 observed with the hydrolysis of phosphate diesters, which is limited by the chemistry step (*29*). Interestingly, the elementary effect observed with Dpo4 is similar to the value of 5.0 observed with correct nucleotide incorporation by rPolβ (*31*). Recent structural and stopped flow fluorescence studies have determined the rate-limiting step of DNA polymerization by rPolβ is in fact the chemistry step (*51*). The combined results from these studies with rPolβ support our results with Dpo4 for a rate-limiting chemistry step for incorrect nucleotide incorporation. Moreover, large elemental effects associated with mismatched nucleotide incorporation have been observed with other polymerases, including T7 DNA polymerase (17−34) (*24*) and *E. coli* DNA polymerase I (65) (*35*). Thus, the assignment of the rate-limiting chemistry step for the incorporation of mismatched nucleotides based on the elemental effect seems to be a general trend for all DNA polymerases. However, a smaller elemental effect (1.9) is observed in the mismatched nucleotide incorporation catalyzed by yPolη (*17*). This exception is not clearly understood. Additional mechanistic evidence other than the elemental effect is needed to evaluate whether the chemistry step limits the incorrect nucleotide incorporation by Dpo4 and yPolη.

REFERENCES

1. Masutani, C., Kusumoto, R., Yamada, A., Dohmae, N., Yokoi, M., Yuasa, M., Araki, M., Iwai, S., Takio, K., and Hanaoka, F. (1999) *Nature 399*, 700−704.
2. Matsuda, T., Bebenek, K., Masutani, C., Hanaoka, F., and Kunkel, T. A. (2000) *Nature 404*, 1011−1013.
3. Levine, R. L., Miller, H., Grollman, A., Ohashi, E., Ohmori, H., Masutani, C., Hanaoka, F., and Moriya, M. (2001) *J. Biol. Chem. 276*, 18717−18721.
4. Bebenek, K., Tissier, A., Frank, E. G., McDonald, J. P., Prasad, R., Wilson, S. H., Woodgate, R., and Kunkel, T. A. (2001) *Science 291*, 2156−2159.
5. Johnson, R. E., Washington, M. T., Haracska, L., Prakash, S., and Prakash, L. (2000) *Nature 406*, 1015−1019.
6. Zhang, Y., Yuan, F., Xin, H., Wu, X., Rajpal, D. K., Yang, D., and Wang, Z. (2000) *Nucleic Acids Res. 28*, 4147−4156.
7. Wang, Z. (2001) *Mutat. Res. 486*, 59−70.
8. Ling, H., Boudsocq, F., Woodgate, R., and Yang, W. (2001) *Cell 107*, 91−102.
9. Li, Y., Korolev, S., and Waksman, G. (1998) *EMBO J. 17*, 7514−7525.
10. Sawaya, M. R., Prasad, R., Wilson, S. H., Kraut, J., and Pelletier, H. (1997) *Biochemistry 36*, 11205−11215.
11. Beese, L. S., Derbyshire, V., and Steitz, T. A. (1993) *Science 260*, 352−355.
12. Huang, H., Chopra, R., Verdine, G. L., and Harrison, S. C. (1998) *Science 282*, 1669−1675.
13. Doublie, S., Tabor, S., Long, A. M., Richardson, C. C., and Ellenberger, T. (1998) *Nature 391*, 251−258.
14. Steitz, T. A. (1999) *J. Biol. Chem. 274*, 17395−17398.
15. Johnson, K. A. (1993) *Annu. Rev. Biochem. 62*, 685−713.

16. Showalter, A. K., and Tsai, M. D. (2002) *Biochemistry 41*, 10571−10576.
17. Washington, M. T., Prakash, L., and Prakash, S. (2001) *Cell 107*, 917−927.
18. Fiala, K. A., and Suo, Z. (2004) *Biochemistry 43*, 2106−2115.
19. She, Q., Singh, R. K., Confalonieri, F., Zivanovic, Y., Allard, G., Awayez, M. J., Chan-Weiher, C. C., Clausen, I. G., Curtis, B. A., De Moors, A., Erauso, G., Fletcher, C., Gordon, P. M., Heikamp-de Jong, I., Jeffries, A. C., Kozera, C. J., Medina, N., Peng, X., Thi-Ngoc, H. P., Redder, P., Schenk, M. E., Theriault, C., Tolstrup, N., Charlebois, R. L., Doolittle, W. F., Duguet, M., Gaasterland, T., Garrett, R. A., Ragan, M. A., Sensen, C. W., and Van der Oost, J. (2001) *Proc. Natl. Acad. Sci. U.S.A. 98*, 7835−7840.
20. Boudsocq, F., Iwai, S., Hanaoka, F., and Woodgate, R. (2001) *Nucleic Acids Res. 29*, 4607−4616.
21. Barshop, B. A., Wrenn, R. F., and Frieden, C. (1983) *Anal. Biochem. 130*, 134−145.
22. Zimmerle, C. T., and Frieden, C. (1989) *Biochem. J. 258*, 381−387.
23. Patel, S. S., Wong, I., and Johnson, K. A. (1991) *Biochemistry 30*, 511−525.
24. Wong, I., Patel, S. S., and Johnson, K. A. (1991) *Biochemistry 30*, 526−537.
25. Donlin, M. J., Patel, S. S., and Johnson, K. A. (1991) *Biochemistry 30*, 538−546.
26. Kati, W. M., Johnson, K. A., Jerva, L. F., and Anderson, K. S. (1992) *J. Biol. Chem. 267*, 25988−25997.
27. Johnson, A. A., and Johnson, K. A. (2001) *J. Biol. Chem. 276*, 38097−38107.
28. Ahn, J., Werneburg, B. G., and Tsai, M. D. (1997) *Biochemistry 36*, 1100−1107.
29. Herschlag, D., Piccirilli, J. A., and Cech, T. R. (1991) *Biochemistry 30*, 4844−4854.
30. Benkovic, S. J., and Schray, K. J. (1971) *Enzymes (3rd Ed.) 8*, 20a.
31. Liu, J., and Tsai, M. D. (2001) *Biochemistry 40*, 9014−9022.
32. Dahlberg, M. E., and Benkovic, S. J. (1991) *Biochemistry 30*, 4835−4843.
33. Eger, B. T., Kuchta, R. D., Carroll, S. S., Benkovic, P. A., Dahlberg, M. E., Joyce, C. M., and Benkovic, S. J. (1991) *Biochemistry 30*, 1441−1448.
34. Bryant, F. R., Johnson, K. A., and Benkovic, S. J. (1983) *Biochemistry 22*, 3537−3546.
35. Kuchta, R. D., Benkovic, P., and Benkovic, S. J. (1988) *Biochemistry 27*, 6716−6725.
36. Kuchta, R. D., Mizrahi, V., Benkovic, P. A., Johnson, K. A., and Benkovic, S. J. (1987) *Biochemistry 26*, 8410−8417.
37. Trincao, J., Johnson, R. E., Escalante, C. R., Prakash, S., Prakash, L., and Aggarwal, A. K. (2001) *Mol. Cell 8*, 417−426.
38. Friedberg, E. C., Fischhaber, P. L., and Kisker, C. (2001) *Cell 107*, 9−12.
39. Ling, H., Boudsocq, F., Plosky, B. S., Woodgate, R., and Yang, W. (2003) *Nature 424*, 1083−1087.
40. Silvian, L. F., Toth, E. A., Pham, P., Goodman, M. F., and Ellenberger, T. (2001) *Nat. Struct. Biol. 8*, 984−989.
41. Zhou, B. L., Pata, J. D., and Steitz, T. A. (2001) *Mol. Cell 8*, 427−437.
42. Yang, W. (2003) *Curr. Opin. Struct. Biol. 13*, 23−30.
43. Johnson, A. A., Tsai, Y., Graves, S. W., and Johnson, K. A. (2000) *Biochemistry 39*, 1702−1708.
44. Kelman, Z. (1997) *Oncogene 14*, 629−640.
45. Gruz, P., Pisani, F. M., Shimizu, M., Yamada, M., Hayashi, I., Morikawa, K., and Nohmi, T. (2001) *J. Biol. Chem. 276*, 47394−47401.
46. Wagner, J., Fujii, S., Gruz, P., Nohmi, T., and Fuchs, R. P. (2000) *EMBO Rep. 1*, 484−488.
47. Haracska, L., Unk, I., Johnson, R. E., Phillips, B. B., Hurwitz, J., Prakash, L., and Prakash, S. (2002) *Mol. Cell. Biol. 22*, 784−791.
48. De Felice, M., Sensen, C. W., Charlebois, R. L., Rossi, M., and Pisani, F. M. (1999) *J. Mol. Biol. 291*, 47−57.
49. Dionne, I., Nookala, R. K., Jackson, S. P., Doherty, A. J., and Bell, S. D. (2003) *Mol. Cell 11*, 275−282.
50. Kokoska, R. J., Bebenek, K., Boudsocq, F., Woodgate, R., and Kunkel, T. A. (2002) *J. Biol. Chem. 277*, 19633−19638.
51. Arndt, J. W., Gong, W., Zhong, X., Showalter, A. K., Liu, J., Dunlap, C. A., Lin, Z., Paxson, C., Tsai, M. D., and Chan, M. K. (2001) *Biochemistry 40*, 5368−5375.

BI035746Z